Design Aspects and Performance Estimation of the Reflector Based Digital Beam-Forming SAR System

A. Patyuchenko, M. Younis, S. Huber, F. Bordoni and G. Krieger

Microwaves and Radar Institute, German Aerospace Center (DLR)
Muenchener Str. 20, 82234 *Wessling, Germany*

Abstract

The paper discusses a novel SAR system concept based on digital beam-forming (DBF) using a reflector antenna. The main design aspects of the reflector antenna with multiple digital feed elements in particular specific for future DBF SAR systems are considered. Based on the presented initial antenna design the system performance is analyzed and the analysis results are discussed.

I. Introduction

Next generation Synthetic Aperture Radar (SAR) systems based on digital beam-forming (DBF) are increasingly studied for future missions [1], [2]. DBF SAR systems will comprise multiple independent channels with analog-to-digital converters and will be free from analog phase and amplitude control elements in the receive chain. This feature in conjunction with DBF techniques allows to achieve an enhanced system performance and, overcoming classical SAR limitations, obtain high resolution wide swath images.

The development process of the DBF SAR entails many challenges and one of the major aspects to be considered here is the radar antenna. Reflector antennas already used in communication and multiple-beam systems have a number of advantages among which are a high directivity and a low-weight deployable structure. All this makes the reflector antenna a candidate for the realization of DBF SAR systems. Some of the open questions in this area are: what are the main reflector design parameters and aspects constrained by overall DBF SAR system requirements, how should they be defined, and what performance can one expect from the reflector based DBF SAR? These questions are answered in the paper. Antenna design aspects specific for this system are considered and discussed. The discussion is followed by the results of the system performance analysis.

II. DBF SAR System: Structure and Operation

A general structure of the SAR system based on the digital beam-forming concept is depicted in Fig. 1. It consists of the reflector antenna, comprised by a circular paraboloid and a feed array, a feed system circuitry and a digital control system. The feed array is represented by primary antennas linearly arranged with a separation d in the reflector's focal plane. Each feed element is connected to a receiving channel represented in a simple form by a Tx/Rx switch, a low noise amplifier, a band-pass filter, and an analog-to-digital converter.

Activation of a single element results in a narrow high-gain beam illuminating a certain portion of the swath. Combination of several channels results in formation of the required antenna pattern. When all the elements are switched on the reflector antenna pattern covers the complete swath by a wide low-gain beam. The given system uses a single digital channel in azimuth and is operated in Scan-On-Receive (SCORE) mode [2], [3]: the ground swath of interest is illuminated by the wide transmit

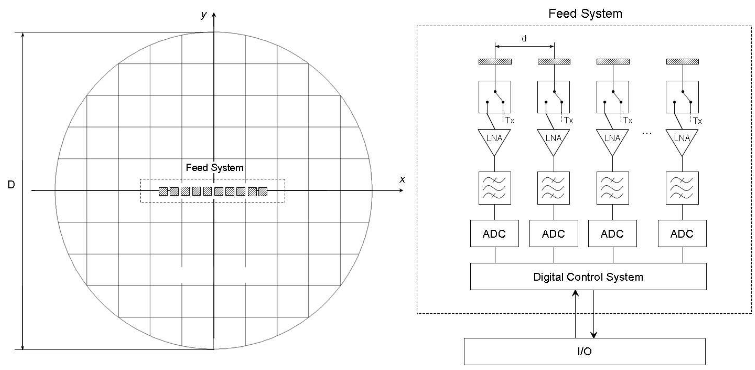

Fig. 1. Simplified architecture of the reflector based DBF SAR system: the reflector dish with a schematically depicted feed system (left) and a simplified structure of the digital feed system circuitry (right).

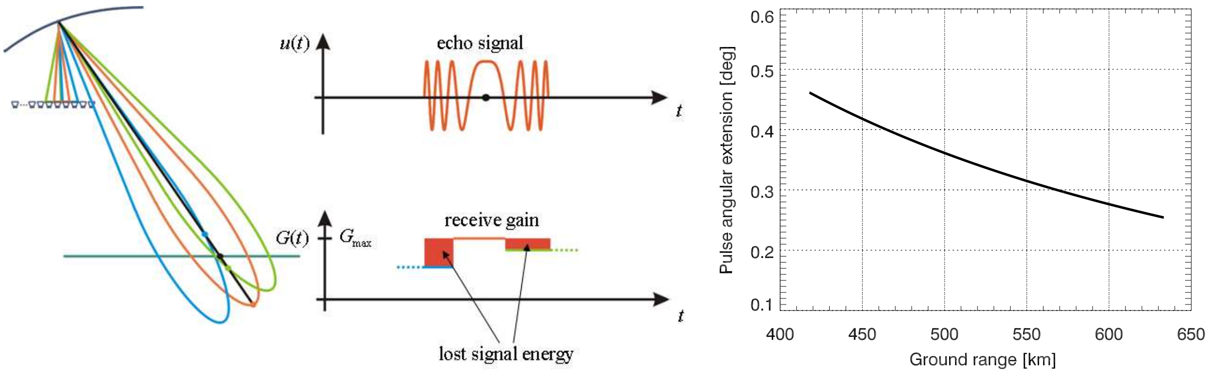

(a) (b)

Fig. 2. a) Pulse extension loss principle. b) Angular pulse extension on ground as a function of ground range.

beam and a narrow receive beam scans over the entire swath following the pulse on ground. The scanning is performed digitally by combining weighted data from the activated signal channels according to the following equation:

$$s_{out}(t) = \sum_{i=1}^{N} w_i(t) \cdot s_{in_i}(t), \tag{1}$$

where N is the total number of elements, $w_i(t)$ are complex weighting coefficients, $s_{in_i}(t)$ is the input signal at the i^{th} channel, $s_{out}(t)$ is the output signal.

An effect which is in particular specific for $SCORE$ operation is the pulse extension effect illustrated in Fig. 2 a). The depicted chirp waveform, $u(t)$, extends in time for the period of pulse duration. During the $SCORE$ operation, when the activated elements are continuously switched, the extended signal returned from a certain look angle is weighted with different antenna patterns and thus with different gains as shown in the lower right of Fig. 2 a) by parallel horizontal lines. This modulation leads to the loss of a signal energy for long pulses and the signal disturbance.

The simplest solution to the problem of long chirp signals is the activation of several elements on receive and the subsequent summation of their output signals which would result in wider Rx patterns. However increasing the number of activated elements the antenna gain may degrade. In this case another, more complex solution, is applicable. Since each feed element at each instant of time receives only a part of a returned signal and therefore only a corresponding part of the signal spectrum, it is possible to split incoming signals from the feeds into multiple sub-bands and to select for each frequency sub-band only the element(s) with the maximum signal power. This method requires more sophisticated digital signal processing. The problem of the pulse temporal extension having an impact on the beam steering mechanism, and the possibility to adapt the position of the beam to the frequency of the received signal are discussed in [4], [2] and [3].

III. Reflector Antenna Design Aspects

In this section reflector antenna design aspects critical for the DBF SAR system are discussed.

A. Transmit/Receive Antenna Beams

The half-power beam width ($HPBW$) of the Tx/Rx antenna patterns must satisfy certain requirements. Required Tx elevation $HPBW$, $\Theta_{Tx_{el}}$, is determined by the swath angular extension, while the Rx azimuth $HPBW$, $\Theta_{Rx_{az}}$, is restricted by the azimuth resolution, δ_a, given by the known relation $\Theta_{Rx_{az}} = \frac{\lambda}{2\delta_a}$, where λ is the operational wavelength. Required Rx elevation $HPBW$, $\Theta_{Rx_{el}}$, is determined by the pulse extension effect. The Rx beam must completely cover the ground projection of the extended pulse expressed by

$$\delta_l = \frac{c_0 \eta}{2PRF \sin\varphi}, \tag{2}$$

where η is the duty cycle, φ is the incidence angle, PRF is the pulse repetition frequency and c_0 is the speed of light. Using (2) the pulse angular extension is plotted as a function of ground range in Fig. 2 b) for the DBF SAR system considered in Section IV. Its value defines the required elevation $HPBW$ of the receive beams which can be achieved by activating and combining several digital channels. It should be noted that the frequency adaptive method, mentioned in Section II, on the other hand imposes no restrictions on the $\Theta_{Rx_{el}}$.

B. Diameter and Focal Length

The required diameter of the reflector antenna is mainly determined by the needed gain and the $HPBW$ of the pattern. However the dependence of these two parameters on the aperture size is different: the larger the reflector the higher its gain but the narrower its $HPBW$. Thus, as long as no use of the advanced DBF techniques mentioned in Section II is made, a certain compromise must be found.

When the transmit power is fixed the gain has a considerable impact on the Noise-Equivalent-Sigma-Zero ($NESZ$) which influences the system radiometric resolution. Therefore an aperture size must be large enough to satisfy the specified $NESZ$ value expressed by:

$$NESZ = \frac{2(4\pi)^3 P_n PRF N_{az} \sin\varphi}{c_0 \lambda^2 P_{av} G_t G_r \delta_{az}} \cdot \Upsilon, \tag{3}$$

where P_n is the noise power, P_{av} is the average transmitted power, N_{az} is the number of integrated pulses during azimuth compression, G_t, G_r are the antenna Tx/Rx gains, c_0 is the speed of light, φ is the incidence angle, λ is the wavelength, δ_{az} is the azimuth resolution, $\Upsilon = f(C_{el}(\theta), C_{az}(\phi), R(\phi,\theta))$ is a function of elevation and azimuth two way antenna patterns and a slant range. Using (3) one can roughly estimate the required antenna gain. Substituting the found value into (4) the corresponding diameter of the ideal reflector can be defined as:

$$D = \frac{\lambda\sqrt{10^{\frac{G_{max}}{10}}}}{\kappa\pi}, \tag{4}$$

where κ is the antenna efficiency. If the found diameter does not satisfy the requirement imposed on the Rx elevation $HPBW$ then the application of one of the afore mentioned solutions is needed to avoid receive signal disturbance due to the finite extension of the chirp signal. In addition the requirement for the Rx azimuth $HPBW$ must be proved.

For the fixed diameter the focal length has an impact on the maximum scan angle as well as on the overall system size. For the maximum allowable gain loss of GL at the maximum scan angle of $\Theta_{Tx_{el}}/2$ we find the focal length using (5) [5] as:

$$F = D \cdot \frac{\pi(\sin\frac{\Theta_{Tx_{el}}}{2} / \sin\frac{\Theta_{HPBW}}{2})}{190(1 - e^{-0.12\sqrt{D/\lambda}}) \cos^{-1}(1 - GL/5)} \tag{5}$$

where Θ_{HPBW} is the $HPBW$ of the reflector antenna pattern when a single feed element is activated in the focal point.

C. Feed System

The feed system is represented by N primary antennas arranged in a linear array with a spacing d in the focal plane of the reflector. The total length of the array, $L \approx (N-1)d$, has an impact on the $HPBW$ and the patterns shape. The reflector antenna was modeled in GRASP9 for several values of N and d. For the found optimum values the transmit pattern satisfies the $HPBW$ requirement with ripples better than $1.5\,\mathrm{dB}$. Formation of the receive beams is performed by sequential activation of two adjacent elements according to the activation matrix shown in Fig. 3 a) as a function of the look angle. This activation matrix allows to achieve the maximum gain and obtain receive patterns satisfying the required $HPBW$ limit.

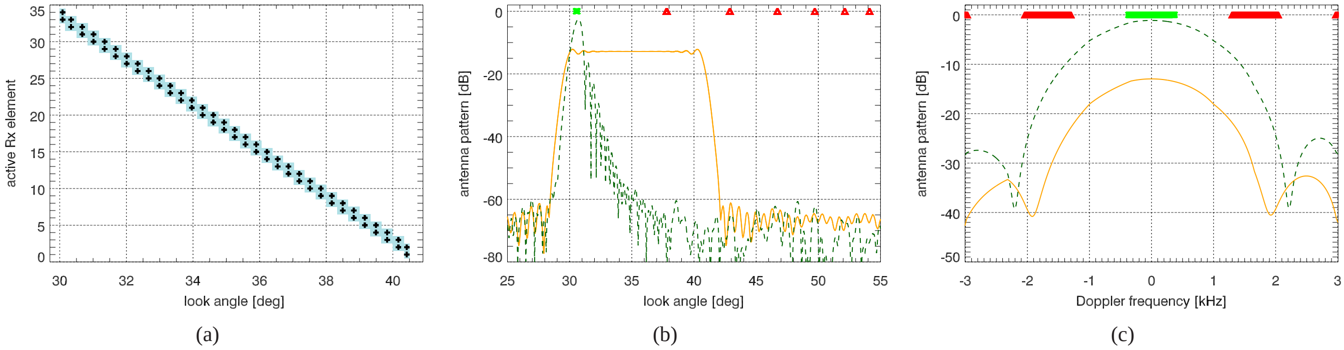

Fig. 3. a) Feed activation matrix as a function of a look angle. b) and c) Elevation and azimuth antenna patterns correspondingly (solid line - Tx, dashed line - Rx).

D. Design Summary

The basic design of the reflector antenna implemented for the DBF SAR system considered in the current work is summarized in Table I a). Patterns of the antenna modeled using the found parameters are depicted in Fig. 3 b) and c) (a feed blockage is not considered). As it will be shown in the next section this initial design requires certain optimization steps aimed at improvement of the overall DBF SAR system performance.

TABLE I

(a) Antenna Parameters

Parameter	Value
operational frequency	$5.3\,\mathrm{GHz}$
diameter	$10\,\mathrm{m}$
focal length	$5.5\,\mathrm{m}$
number of elements	34
inter-element spacing	$0.6 \cdot \lambda$

(b) System Requirements ans Specifications

Parameter	Value
average transmitted power	$170\,\mathrm{W}$
duty cycle	$\eta = 5\%$
bandwidth	$25\,\mathrm{MHz}$
resolution	$\leq 8\,\mathrm{m}$
$NESZ$, $RASR$	$\leq -30\,\mathrm{dB}$
ground swath width	$212\,\mathrm{km}$
repeat cycle	13 days
look angles	$30^\circ - 40.5^\circ$
orbit height	$710\,\mathrm{km}$

IV. Reflector Based DBF SAR Performance

This section considers performance analysis results of the DBF SAR system based on the designed reflector antenna and discusses the problem of system optimization. In Table I b) the main requirements and specifications of the system are summarized. The timing diagram is shown in Fig. 4 f) where the swath of interest is depicted by two vertical stripes with an in-between gap representing blind ranges.

A. Performance Analysis Results

Range- and Azimuth-Ambiguity-to-Signal Ratio ($RASR$, $AASR$): $AASR$ quantifies the aliasing generated by the finite sampling of the Doppler spectrum at intervals of the pulse repetition frequency (PRF), while $RASR$ characterizes the disturbance due to the echoes from preceding and succeeding pulses which arrive simultaneously with the echo of interest. The system performance in terms of $AASR$ and $RASR$ is presented in Fig. 4 a) and b) correspondingly. The processed Doppler bandwidth of $748\,\mathrm{Hz}$ is indicated in Fig. 3 c) by the central horizontal bar located at the top of the plot, and the ambiguous spectral domains are depicted by the off-center bars. The overall azimuth ambiguities level over the swath is below $-15\,\mathrm{dB}$ while the achieved azimuth resolution is around $8\,\mathrm{m}$.

When considering the level of range ambiguities, the PRF has an opposite effect as for the azimuth ambiguities. The higher the PRF the lower the level of $AASR$ but the higher the level of $RASR$. As it can be seen from the small triangles on the top of Fig. 3 b), all the ambiguities are outside the main lobe of the two way antenna pattern. This results in a good suppression of range ambiguities which are well below $-30\,\mathrm{dB}$.

Noise-Equivalent-Sigma-Zero ($NESZ$): $NESZ$ is a measure of the sensitivity of the SAR system. The $NESZ$ as a function of ground range is shown in Fig. 4 c). The degradation of $NESZ$ in the far ranges of the swath is due to the larger free space attenuation of the signal. The discontinuities in the curve are due to the switching of elements resulting in discrete patterns. It should be noted that a non-ideal reflector antenna with a net efficiency of 0.7 would introduce additional losses leading to an increase of the $NESZ$ by around 3 dB.

Relative Peak-to-Side Lobe Ratio ($PSLR$) and Peak Ratio: Relative $PSLR$ and Peak Ratio are measures of the distortion of the received signal due to the finite extension of the chirp and the switching of the feed elements discussed in Section II. They are defined for the received chirp signal at the output of a matched filter such that: Relative $PSLR$ is the ratio of the peak amplitude to the first side lobe level of the signal relative to the ratio of the ideal case when the chirp signal is not modulated. On the other hand, Peak Ratio is the amplitude ratio of modulated and non-modulated signals. Relative $PSLR$ and Peak Ratio for the given DBF SAR are shown in Fig. 4 d) and e) correspondingly. These characteristics are the result of the system impulse response analysis. The increased Peak Ratio at the swath borders is due to the gain loss of the antenna when the elements out of the focal point are activated. This effect is included here since the amplitude of the ideal non-modulated signal is one.

B. Design Optimization Notes

Based on the above results one can conclude that the overall system performance can be improved by optimizing the initial reflector antenna design presented in this paper. For example, the increase of the level of azimuth ambiguities at the swath edges is due to the wider azimuth antenna patterns formed by the activation of the elements at extremes. In this case the ambiguous spectral domains are falling more into the main lobe thus making $AASR$ worse. The straight forward solution to this problem is the increase of PRF value which should be no problem regrading the $RASR$ and the timing diagram. The further improvement of the overall level of azimuth ambiguities can be achieved by changing the reflector design and improving azimuth patterns of the antenna. Relative $PSLR$ and Relative Peak can be improved by the reduction of the pulse length which in this case should also be no problem since the $NESZ$ performance is quite good exceeding typical requirements. The second

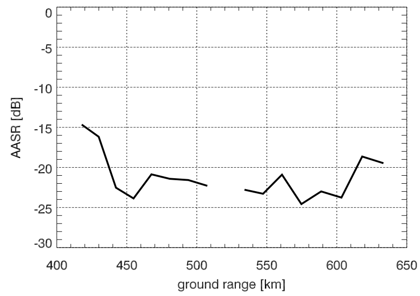

(a) AASR

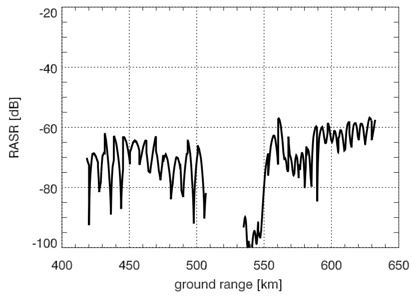

(b) RASR

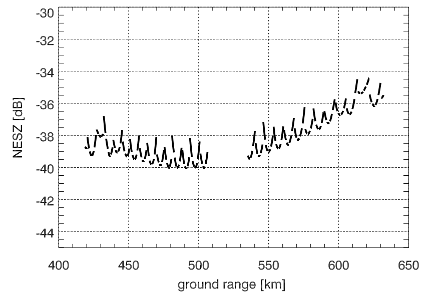

(c) NESZ

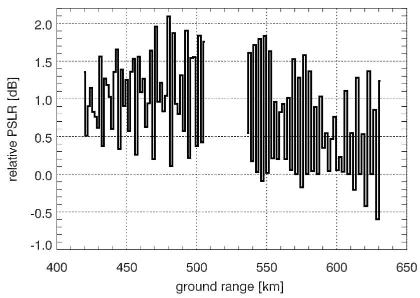

(d) Relative PSLR

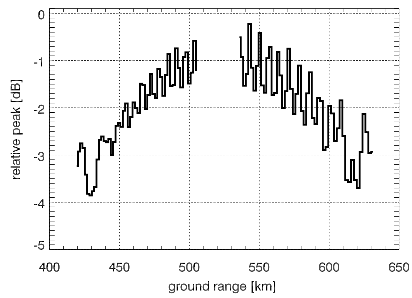

(e) Relative Peak

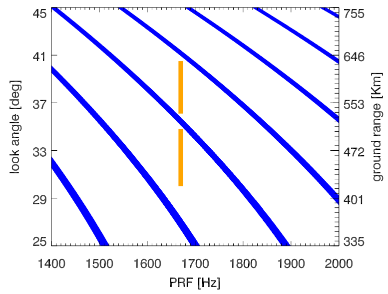

(f) Timing diagram

Fig. 4. DBF SAR System Performance and the timing diagram.

optimization step aimed at the further reduction of the pulse extension effect is the use of wider beams in elevation. This could be achieved by activating more elements on receive. But since this solution in conjunction with the initial antenna design would result in the gain loss and thus in the increase of the $NESZ$ level, an additional optimization of the antenna would be needed again (an alternative solution here could be the use of more sophisticated digital signal processing algorithms to avoid the losses due to the finite pulse extension).

An important effect which was not considered in this work is the frequency dependence of the antenna patterns. This effect has an impact on the DBF SAR system performance and might be considerably increased by blockage effects. In this case an optimization of the initial reflector design and reduction of the feed blockage effect would also improve the overall system performance.

V. Conclusion

A novel idea of combining a reflector antenna with a digital feed system as suggested in [6] is detailed, and the main system specific antenna design aspects are discussed. The presented reflector based digital beam-forming SAR system has a number of advantages in comparison, e.g. with a future planar based DBF SAR [6]. The large aperture results in a high ambiguity suppression as well as in an increase of the radiometric resolution which is demonstrated by the presented analysis. At the same time, a light-weight unfoldable reflector can be compactly placed on board of a launcher. The feed activation algorithm can be fully automatized which would ease the instrument commanding and avoid the beam steering loss from topographic height induced mispointings. However the finite extension of the transmitted chirp may require more sophisticated digital signal processing.

The results of the current work showed that combination of the reflector antenna with a future digital beam-forming SAR system is a promising concept allowing to achieve an outstanding performance while keeping a system complexity on a relatively low level.

References

[1] G. Krieger, N. Gebert, and A. Moreira, “Multidimensional waveform encoding for synthetic aperture radar remote sensing,” *IEEE Transactions on Geoscience and Remote Sensing*, vol. 46, no. 1, pp. 31–46, Jan. 2008.

[2] M. Suess and W. Wiesbeck, “Side looking SAR system,” Patent 20 040 150 547, Mar. 30, 2004.

[3] B. G. M. Suess and R. Zahn, “A novel high resolution, wide swath SAR,” in *Proc. Int. Geoscience and Remote Sensing Symposium (IGARSS’01)*, vol. 3, 2003, pp. 1013–1015.

[4] J. T. Kare, “Moving receive beam method and apparatus for synthetic aperture radar,” Patent 6 175 326, Jan. 16, 2001.

[5] S.-W. Lee and Y. Rahmat-Samii, “Simple formulas for designing an offset multibeam parabolic reflector,” *IEEE Transactions on Antennas and Propagation*, vol. AP-29, no. 3, pp. 472–478, May 1981.

[6] M. Younis, S. Huber, A. Patyuchenko, F. Bordoni, and G. Krieger, “Performance comparison of reflector- and planar-antenna based digital beam-forming SAR,” International Journal of Antennas and Propagation (Special Issue on Active Antennas for Space Applications), 2009, submitted, to be published.